

An evolutionary missing link? A modest-mass early-type galaxy hosting an over-sized nuclear black hole

Jacco Th. van Loon¹ and Anne E. Sansom²

¹Lennard-Jones Laboratories, Keele University, Staffordshire ST5 5BG, UK

²Jeremiah Horrocks Institute, University of Central Lancashire, Preston PR1 2HE, UK

2015

ABSTRACT

SAGE1C J053634.78–722658.5 is a galaxy at redshift $z = 0.14$, discovered behind the Large Magellanic Cloud in the *Spitzer* Space Telescope “Surveying the Agents of Galaxy Evolution” Spectroscopy survey (SAGE-Spec). It has very strong silicate emission at $10\ \mu\text{m}$ but negligible far-IR and UV emission. This makes it a candidate for a bare AGN source in the IR, perhaps seen pole-on, without significant IR emission from the host galaxy. In this paper we present optical spectra taken with the Southern African Large Telescope (SALT) to investigate the nature of the underlying host galaxy and its AGN. We find broad $\text{H}\alpha$ emission characteristic of an AGN, plus absorption lines associated with a mature stellar population (> 9 Gyr), and refine its redshift determination to $z = 0.1428 \pm 0.0001$. There is no evidence for any emission lines associated with star formation. This remarkable object exemplifies the need for separating the emission from any AGN from that of the host galaxy when employing infrared diagnostic diagrams. We estimate the black hole mass, $M_{\text{BH}} = 3.5 \pm 0.8 \times 10^8 M_{\odot}$, host galaxy mass, $M_{\text{stars}} = 2.5_{1.2}^{2.5} \times 10^{10} M_{\odot}$, and accretion luminosity, $L_{\text{bol}}(\text{AGN}) = 5.3 \pm 0.4 \times 10^{45} \text{ erg s}^{-1}$ (≈ 12 per cent of the Eddington luminosity) and find the AGN to be more prominent than expected for a host galaxy of this modest size. The old age is in tension with the downsizing paradigm in which this galaxy would recently have transformed from a star-forming disc galaxy into an early-type, passively evolving galaxy.

Key words: quasars: individual: SAGE1C J053634.78–722658.5 – quasars: supermassive black holes – galaxies: individual: [GC2009] J053642.29–722556.6 – galaxies: peculiar – galaxies: active – stars: individual: [VS2015] J053640.54–722615.5

1 INTRODUCTION

Active Galactic Nuclei (AGN) result from accretion of gas by a supermassive black hole in the centre of a galaxy. AGN have been found in spiral galaxies and massive elliptical galaxies, but whilst it may be assumed that all spiral and massive elliptical galaxies harbour a supermassive black hole they do not all exhibit the same level of nuclear activity. AGN activity is linked to the assembly history of galaxies, with massive galaxies evolving faster. A result is the intimate link between the mass of the black hole and that of the host galaxy’s spheroidal component (Kormendy & Ho 2013; Graham 2015).

The current paradigm dictates that AGN manifest themselves in different guises depending on the angle under which they are seen (Netzer 2015): the broad emission-line region (BLR) in the dense, fast-rotating inner part of the AGN is obscured from view by a dusty torus if seen under a high inclination; this leaves exposed a narrow emission-line region (NLR). When the nucleus is seen more directly,

then the optical emission has a strong continuum component obliterating the NLR – these so-called “blazars” are relatively faint at far-infrared (far-IR) wavelengths.

SAGE1C J053634.78–722658.5 (hereafter referred to as “SAGE0536AGN”) is an AGN which was serendipitously discovered by Hony et al. (2011, hereafter H11) in the *Spitzer* Space Telescope Survey of the Agents of Galaxy Evolution Spectroscopic followup of IR sources seen towards the Large Magellanic Cloud (SAGE-Spec: Kemper et al. 2010; Woods et al. 2011). Its peculiarity, and reason to have found its way into the SAGE-Spec target list, is due to its spectral energy distribution (SED) peaking at mid-IR wavelengths; the low-resolution *Spitzer* spectrum revealed the strongest silicate emission of any known AGN (H11). It is faint at optical wavelengths, ~ 17 – 18 mag, and not detected at far-IR wavelengths, 70 – $160\ \mu\text{m}$, but radio loud (see H11 for a summary of measurements). H11 used the weak mid-IR emission bands that are generally attributed to Polycyclic Aromatic Hydro-carbons (PAHs) to estimate a red-

shift $z = 0.140 \pm 0.005$. They suggest the near-IR continuum arises from hot dust near the accretion disc whilst the silicate emission originates further out in dusty clouds within ~ 10 pc from the black hole. Silicate would appear in emission either if the torus is transparent and/or clumpy, or the viewing angle is close to pole-on.

The unique character of this object merits further study, in particular aimed at detecting the BLR and/or NLR and to determine the nature of its host galaxy. We here present answers to those questions based on the first optical spectroscopy of this intriguing AGN, which we obtained with the Southern African Large Telescope (SALT).

2 OBSERVATIONS AND DATA PROCESSING

The observations reported here were obtained with SALT (Buckley, Swart & Meiring 2006) under programmes 2012-1-UKSC-002 & 2013-1-UKSC-007 (PI: van Loon). With an 11×10 m² segmented spherical primary mirror across which the pupil is tracked, SALT is the largest single optical telescope in the world. It is situated at the South African Astronomical Observatory (SAAO) site in the interior of the Northern Cape province in the Republic of South Africa, at an altitude of 1800m. We made use of the Robert Stobie Spectrograph (RSS; Burgh et al. 2003; Kobulnicky et al. 2003) in its long-slit mode. The details of the observations are summarised in Table 1. The signal was sampled by 2×2 detector elements upon read-out, to limit electronic noise whilst adequately sampling the spectral and angular resolution elements. Two gaps appear in the spectrum because of the physical separation between the three detectors.

The slit was oriented 32° east from north – roughly aligned with the *Spitzer* InfraRed Spectrograph’s short-wavelength slit and perpendicular to its much wider long-wavelength slit (cf. H11) – so as to overlap with an anonymous star and a resolved galaxy (narrowly missing its nucleus). The star, which we name [VS2015] J053640.54–722615.5 (hereafter “SAGE0536S”), is optically brighter than the target AGN and was deemed useful to cancel telluric absorption in the spectrum of the target. The galaxy, [GC2009] J053642.29–722556.6 (hereafter “SAGE0536G”) was discovered, also serendipitously, by Gruendl & Chu (2009) in their search for young stellar objects in the *Spitzer* SAGE-LMC photometric survey (Meixner et al. 2006). SAGE0536G is bright at UV, mid- and far-IR wavelengths but not particularly bright at radio frequencies (see Fig. 1 in H11, where it is the brightest object at 8–160 μ m).

All data were processed using the PySALT software suite (Crawford et al. 2010), as follows: (i) preparation for the subsequent procedures using the task SALTPREPARE; (ii) correction for gain differences between the amplifiers of the different detectors using the task SALTGAIN; (iii) correction for cross-talk between the amplifiers upon read-out of the detectors using the task SALTXTALK; (iv) correction for the electronic off-set by subtracting the bias level determined from the un-illuminated part of the detector using the task SALTBIAS; (v) cleansing the majority of cosmic ray imprints using the task SALTFCLEAN; (vi) mosaicking into a single frame using the task SALTMOAIC. We derived a wavelength solution from the exposure of an argon arc lamp which had

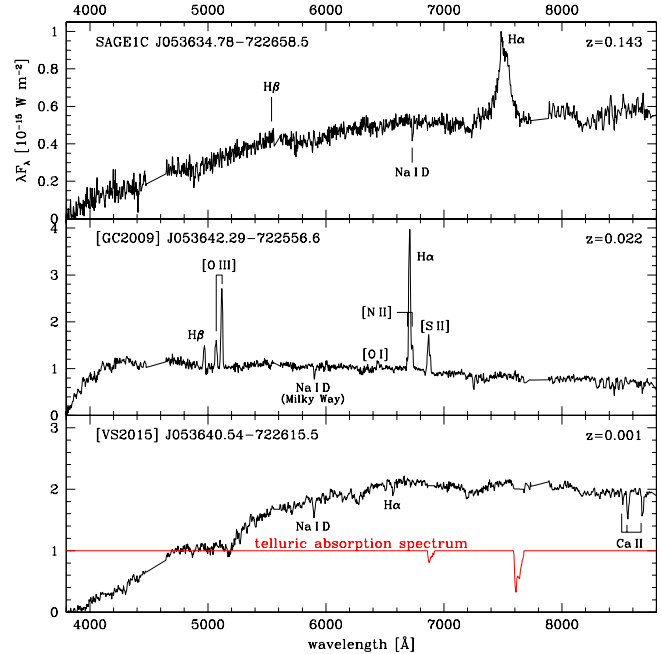


Figure 1. SALT-RSS spectra of the (*top*) AGN, (*middle*) galaxy, and (*bottom*) star at low resolution covering most of the optical range. Conspicuous spectral features are labelled. The spectra have *not* been corrected for redshift.

been taken immediately after the science exposure, using the interactive task SPECIDENTIFY. This was then applied to the science frames using the task SPECRECTIFY. In the case of multiple exposures these were combined using the task SALTCOMBINE. The tasks SPECSKY and SPECXTRACT were used, respectively, to subtract background light determined from a patch of sky adjacent to the object of interest and to extract a weighted average of the rows on the detector covering the object of interest.

The standard star EG 21 was observed on the 8th of September 2012 with a $4''$ -wide slit but otherwise identical instrumental set-up. The data were processed in the same fashion as described previously, before determining a 3rd-order polynomial response function using the task SPECCAL, which also includes a correction for the atmospheric continuum extinction but not discrete telluric features. The latter were removed by division by a normalised template incorporating two telluric oxygen bands as observed in the spectrum of SAGE0536S. Artefacts remaining from imperfect removal of cosmic rays and telluric emission were removed manually.

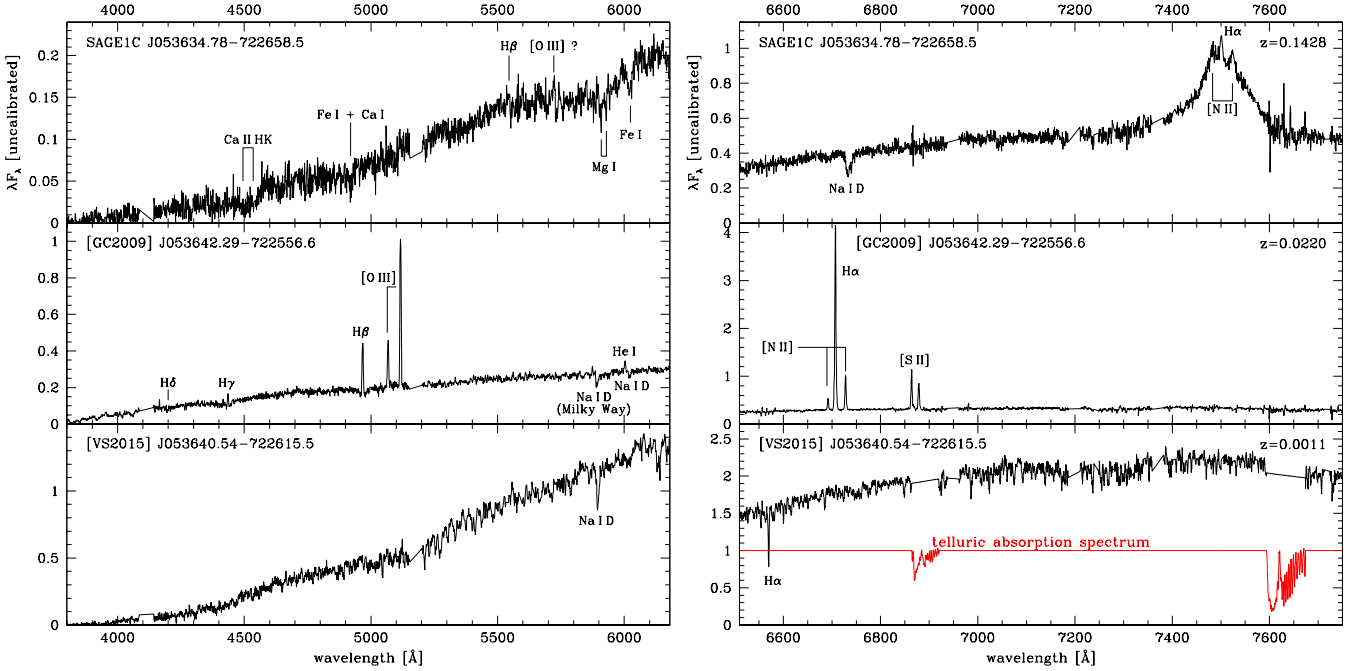
3 SCIENTIFIC RESULTS

3.1 Overall spectral appearance: the nature of the AGN host galaxy

Figures 1 & 2 show the spectra of SAGE0536AGN, G and S. The first observation one could make is that SAGE0536AGN exhibits broad H α emission, SAGE0536G displays narrow Balmer and forbidden line emission, whilst SAGE0536S only shows absorption lines. Secondly, SAGE0536AGN is redshifted with respect to SAGE0536G, which is redshifted with

Table 1. Observing parameters.

dd/mm/yy	grating/filter	slit	$R = \lambda/\delta\lambda$	grating/camera angle	$\Delta\lambda$ (Å)	t_{int} (min)	airmass	seeing
08/09/12	PG0300/PC03850	1''25 × 8'	300–700	5°38/10°74	3800–10400	1 × 9	2.12	1''2
11/10/12	PG1800/PC04600	1''25 × 8'	3400–4000	40°25/80°51	6500–7750	3 × 16	1.33	1''9
24/09/13	PG0900/(no filter)	1''00 × 8'	1000–1500	12°12/24°25	3800–6180	3 × 13	1.32	2''0


Figure 2. As Fig. 1, but: (*left*) at medium resolution covering the blue–orange and (*right*) at high resolution covering the red portion.

respect to SAGE0536S. We thus identify SAGE0536AGN as an AGN, SAGE0536G as a star-forming galaxy, and SAGE0536S as a cool star.

The weakness of any narrow emission lines, in particular of [O III], in the spectrum of SAGE0536AGN is of significance as it means there is next to no current star formation activity. This is consistent with the lack of far-IR emission (H11), and implies that we are dealing with an early-type galaxy. Indeed, the lack of strong Balmer absorption lines but presence of metal absorption lines implies the absence of a sizeable population of stars younger than a few Gyr. The jump in the spectrum around a restwavelength of 4000 Å, $D_n(4000)$ (Balogh et al. 1999) and the $H\delta$ line index, $H\delta_A$ (Worthey & Ottaviani 1997) can be used as age indicators. We estimate $D_n(4000) \sim 1.91$ and $H\delta_A \sim -0.09$ Å, which (including the look-back time – see below) would correspond to a dominant age of ~ 9 Gyr, or even older for sub-solar metallicity (Kauffmann et al. 2003a).

The broad $H\alpha$ emission in SAGE0536AGN is superimposed with weak, narrow line emission from $H\alpha$ and [N II]. The dominance of the BLR over the NLR suggests that the orientation of SAGE0536AGN is such that we have a clear view of the central engine, unobstructed by the dusty torus that governs the IR emission (cf. Antonucci & Miller 1985; Antonucci 1993; Urry & Padovani 1995; Beckmann & Shriver 2012). The narrow $H\alpha$ and [N II] lines are about equally strong; this already suggests an AGN origin (Bald-

win, Phillips & Terlevich 1981; Kauffmann et al. 2003a). While detection of the [O III] line is highly uncertain it may be about twice as bright as the narrow $H\beta$ line (Fig. 2). This would place it among the LINERS (Kewley et al. 2001; Kauffmann et al. 2003a).

3.2 Kinematics: galaxy redshift, galaxy mass and black hole mass

The recession velocity of SAGE0536AGN results in a redshift $z = 0.1428 \pm 0.0001$, which corresponds to a distance of 700 Mpc, k-corrected distance modulus of 39.08 mag and a look-back time of 1.86 Gyr according to the standard Λ -CDM model with Hubble constant $H_0 = 67.8$ km s $^{-1}$ Mpc $^{-1}$ and matter density $\Omega_0 = 0.308$ (cf. Planck Collaboration 2015). This redshift value is consistent with the estimate from the PAH features in the mid-IR (H11). This confirms that the optical object is the same as the IR object. The other galaxy, SAGE0536G has a redshift $z = 0.0220 \pm 0.0001$ (a distance of 100 Mpc); the line emission shows a gradient along the slit of $\sim \pm 20$ km s $^{-1}$, presumably due to the (projected) rotation of the disc of this galaxy. The redshift of the star, SAGE0536S is $z = 0.0011 \pm 0.0001$, which places it within the LMC.

The stellar velocity dispersion in SAGE0536AGN was determined with the PPF software (Cappellari & Emsellem 2004) to fit a spectrum of a Lick standard star (HD 6203) to

the 5695–6070 Å rest wavelength spectral region. HD 6203 had been observed using the PG1300 grating but with an 0".6 slit and hence a spectral resolution that matches well that of our PG1800 spectrum. The Na I D is by far the most conspicuous stellar feature in the spectrum of SAGE0536AGN and drives the value for the velocity dispersion, $\sigma = 123 \pm 15$ km s⁻¹. This makes it a modest-mass galaxy, and intermediate-mass for an early-type galaxy – $M_{\text{stars}} \sim 2.5 \times 10^{10} M_{\odot}$ accurate to within about a factor two based on the uncertainty in the velocity dispersion and spread in the $M_{\text{stars}}-\sigma$ relation (Wake, van Dokkum & Franx 2012; Cappellari et al. 2013; Belli, Newman & Ellis 2014). The visual brightness is $V \sim 18$ mag (estimated from the B- and i-band photometry in H11), hence $L(V) \sim 2 \times 10^{10} L_{\odot}$.

As motions within the BLR are dominated by the gravitational well of the central black hole, the H β line profile yields an estimate of the black hole mass (Kaspi et al. 2000; Vestergaard & Peterson 2006). Because of the faintness of the H β emission we use instead the H α line, which has a Full Width at Half Maximum (FWHM) $\sim 4000 \pm 400$ km s⁻¹ (corresponding to a Gaussian $\sigma \sim 1700$ km s⁻¹). Following Woo et al. (2014), who present a relation for the black hole mass derived solely from the H α line profile for type I AGNs:

$$\frac{M_{\text{BH}}}{M_{\odot}} = 2.2 \times 10^7 \times \left[\frac{\sigma(\text{H}\alpha)}{10^3 \text{ km s}^{-1}} \right]^{2.06} \left[\frac{L(\text{H}\alpha)}{10^{42} \text{ erg s}^{-1}} \right]^{0.46} \quad (1)$$

The H α luminosity is estimated from the integrated line profile and the i-band magnitude (H11) – $L(\text{H}\alpha) \sim 4 \pm 0.4 \times 10^{43}$ erg s⁻¹. Hence, $M_{\text{BH}} \sim 3.5 \pm 0.8 \times 10^8 M_{\odot}$.

3.3 Foreground interstellar absorption

The spectrum of SAGE0536G shows absorption in the Na I D doublet at 5890+5896 Å, arising within the interstellar medium of the Milky Way and/or LMC (van Loon et al. 2013); foreground absorption in the diffuse interstellar band at 4428 Å is uncertain as it would coincide with redshifted Br γ arising in SAGE0536G. Likewise, any foreground Na I D absorption in the spectrum of SAGE0536AGN would coincide with redshifted Mg I whilst in the spectrum of SAGE0536S it would coincide with the stellar photospheric Na I D absorption.

4 DISCUSSION ON THE NATURE OF SAGE0536AGN

4.1 The host galaxy

The brightness of SAGE0536AGN at radio, compared to that at optical frequencies, $F_{\nu}(4.75 \text{ GHz})/F_{\nu}(\text{B}) = 40 \text{ mJy}/0.162 \text{ mJy} \gg 10$ makes it a radio-loud AGN (Kellermann et al. 1989). On the other hand, $L_{\nu}(178 \text{ MHz}) \sim 4 \times 10^{21} \ll 2 \times 10^{25} \text{ W Hz}^{-1} \text{ sr}^{-1}$ places it in the Fanaroff–Riley class I (Fanaroff & Riley 1974); SAGE0536AGN may well have the bright radio lobes that are characteristic of radio-loud galaxies, but if viewed close to pole-on it may resemble a compact FR-I type radio source.

The faintness at optical wavelengths ($M_{\text{B}} = -20.6$ mag) and brightness at X-ray frequencies ($L_{\text{X}}(0.1\text{--}2.4 \text{ keV}) = 1.5 \times 10^{43}$ erg s⁻¹ – see H11), and relative strength of broad

Table 2. WISE photometry for SAGE0536AGN (from Cutri et al. 2014); magnitudes are on the Vega system and flux densities are isophotal assuming $F_{\nu} \propto \nu^{-2}$ and have not been colour-corrected.

band	λ (μm)	magnitude	F_{ν} (mJy)
W1	3.4	12.404 \pm 0.024	3.4
W2	4.6	11.386 \pm 0.021	4.8
W3	12	8.610 \pm 0.020	11.4
W4	22	6.607 \pm 0.043	19.0

compared to narrow Balmer lines, places SAGE0536AGN in the category of Seyfert 1 (Schmidt & Green 1983; Osterbrock 1977, 1981). While elliptical galaxies are the typical host of a broad-line radio AGN, most Seyferts are radio-quiet AGN residing in spiral galaxies. There thus seems to be some ambiguity as to the expected host galaxy type of SAGE0536AGN, which we have shown here is of early-type and definitely not a spiral galaxy. Indeed, in the diagnostic diagram of H α equivalent width versus [N II]/H α ratio – which Cid Fernandes et al. (2010) introduced to circumvent problems with weak or absent H β and/or [O III] lines which traditionally form part of line diagnostic diagrams – SAGE0536AGN has much weaker [N II] than is usual for Seyferts. However, this is probably because we are comparing the [N II] from the NLR with the H α from the BLR.

The UV-to-IR ratio is different for early- and late-type galaxies. SAGE0536AGN was not detected at near-UV (NUV) wavelengths with GALEX, however, to a limit of 3 μJy (H11). Following Fukugita et al. (1996) this corresponds to an AB magnitude of 7.07, and hence the NUV–[3.6] colour is > 5 mag. According to Bouquin et al. (2015) this makes SAGE0536AGN most likely an elliptical or S0 galaxy. So this is consistent with our optical spectroscopic determination of the galaxy type.

Near-IR colours are not very discriminative, with the $J - K_{\text{s}} \sim 2$ mag of SAGE0536AGN placing it among moderately obscured AGN that include a wide range of host galaxy and AGN types (Rose et al. 2013). Mid-IR colours, however, can distinguish between different kinds of objects, as LaMassa et al. (2013b) have demonstrated using WISE data. SAGE0536AGN was in fact detected in all four WISE bands (Table 2; Cutri et al. 2014). According to Fig. 11 in LaMassa et al. (2013b) and Fig. 5 in Cluver et al. (2014) this firmly places SAGE0536AGN among the QSOs, i.e. a galaxy dominated by its AGN. Indeed, the mid-IR flux densities roughly follow a powerlaw $F_{\nu} \propto \nu^{-0.92}$ rather than a black-body (cf. Yang, Chen & Huang 2015). The dominance of the AGN over emission from the host galaxy may be a reason why the usual diagnostics based on optical, X-ray and radio data yield ambiguous expectations for the galaxy type of SAGE0536AGN. Even mid-IR diagrams are not without ambiguity; in the WISE [4.6]–[12] versus galaxy mass diagram of Alatalo et al. (2014) the sequences of early-type (blue [4.6]–[12] colours) and late-type (red [4.6]–[12] colours) galaxies separate very well yet SAGE0536AGN would clearly – and mistakenly – end up among the late-type galaxies (and optical ‘green valley’ galaxies) because its AGN dominates over the host galaxy.

The lack of far-IR emission places stringent constraints, not only on the star formation rate but also on the mass of

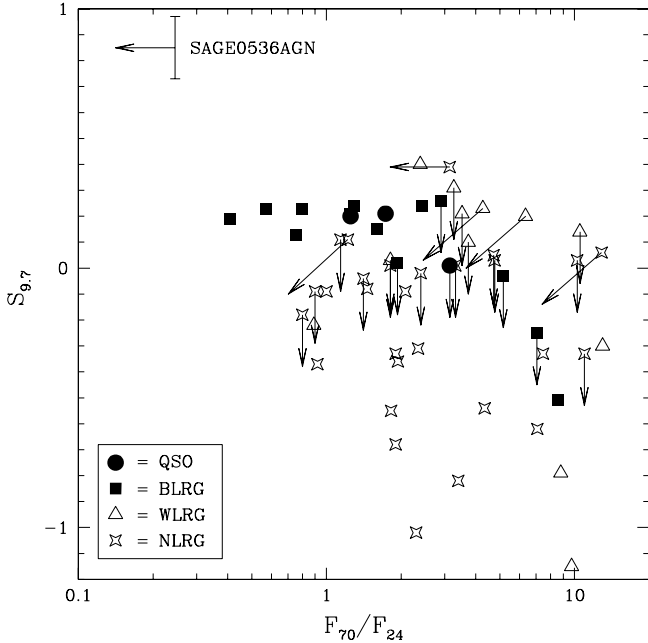


Figure 3. Silicate strength $S_{9.7}$ versus F_{70}/F_{24} flux ratio for narrow-line, weak-line and broad-line radio galaxies and QSOs (Dicken et al. 2008, 2010, 2014) and SAGE0536AGN.

interstellar gas. Groves et al. (2015) found relations between the total interstellar hydrogen mass and the luminosity in *Herschel* Space Observatory bands, for a sample of mostly irregular and spiral galaxies. The strongest constraint on the gass mass in SAGE0536AGN is set by the 160- μm 3- σ upper limit of 4 mJy (H11), yielding $M_{\text{gas}} < 10^9 M_{\odot}$ (according to Groves et al. 2015). With $M_{\text{gas}}/M_{\text{stars}} < 0.1$ this implies it is gas-poor, as expected for an early-type galaxy. The corresponding limit on the star formation rate is (Willott, Bergeron & Omont 2015) $< 1.5 \times 10^{-10} L_{\text{FIR}}(L_{\odot}) \sim 0.26 M_{\odot} \text{ yr}^{-1}$ or a specific star formation rate $< 1.3 \times 10^{-11} \text{ yr}^{-1}$ – clearly below that on the main sequence of star-forming galaxies (Wuyts et al. 2012; Vulcani et al. 2015; Renzini & Peng 2015).

The narrow $\text{H}\alpha$ emission component has an equivalent width $\sim 1.7 \text{ \AA}$ (accurate to ~ 10 per cent). Following Hopkins et al. (2003), for an R-band magnitude ≈ 17.5 (estimated from the B-band and i-band photometry in H11) and the measured Balmer decrement (see below) and redshift, this would yield $L_{\text{H}\alpha} \sim 3.4 \times 10^{35} \text{ W}$ (accurate to within about a factor two). If this were due to star formation activity then, following Wijesinghe et al. (2011), the star formation rate would be $\sim 10 M_{\odot} \text{ yr}^{-1}$. The fact that this is forty times above the upper limit derived from the far-IR luminosity means that the narrow $\text{H}\alpha$ emission component must be associated with the NLR of the AGN instead.

4.2 The central engine

SAGE0536AGN stands out by its extremely strong silicate emission at 9.7 μm . Strong silicate emission is typical of broad-line radio galaxies (Dicken et al. 2014), so our BLR-dominated optical spectrum is consistent with its known radio loudness (H11). However, while its F_{20}/F_7 flux ratio (estimated from the *Spitzer* spectrum at 7 and 20 μm)

is not unusual for this kind of galaxy/AGN, it takes an extreme position in a diagram of silicate strength ($S_{9.7} = \ln(F_{9.7}/F_{\text{continuum}})$ – Spoon et al. 2007) versus F_{70}/F_{24} flux ratio (Fig. 3) compared to a sample of radio galaxies with *Spitzer* spectroscopy (Dicken et al. 2014). SAGE0536AGN shares the characteristics of strong silicate emission and low F_{70}/F_{24} flux ratio with BLR galaxies, which is consistent with its optical spectrum being dominated by BLR emission. However, it is more extreme than the BLR galaxies featuring in this plot both in its silicate emission *and* in its F_{70}/F_{24} flux ratio. It is possible that this is related to its modest host galaxy mass, compared to that of the comparison sample of BLR galaxies.

Gandhi et al. (2009) have shown that an excellent relation exists between the spatially resolved mid-IR luminosity of a Seyfert-type AGN and its X-ray luminosity. We could consider whether the same relationship might also apply to SAGE0536AGN. With an estimated foreground (Galactic + LMC) hydrogen column density of $N(\text{H}) \approx 1 \times 10^{21} \text{ cm}^{-2}$ (Staveley-Smith et al. 2003), and assuming a photon index of 2 (P.Gandhi, private communication) we use the ROSAT measurement (see H11) and the PIMMS tool¹ to estimate that $L_{\text{X}}(2-10 \text{ keV}) \sim 1.8 \times 10^{43} \text{ erg s}^{-1}$. According to the relation in Gandhi et al. (2009)

$$\log \left[\frac{L_{\text{IR}}(12.3 \mu\text{m})}{10^{43} \text{ erg s}^{-1}} \right] = 0.19 + 1.11 \log \left[\frac{L_{\text{X}}(2-10 \text{ keV})}{10^{43} \text{ erg s}^{-1}} \right] \quad (2)$$

this would predict $L_{\text{IR}}(12.3 \mu\text{m}) \sim 3 \times 10^{43} \text{ erg s}^{-1}$. The observed mid-IR luminosity of SAGE0536AGN is $L_{\text{IR}}(12.3 \mu\text{m}) \sim 1.3 \times 10^{44} \text{ erg s}^{-1}$, i.e. a factor ~ 4 brighter. We could reconcile the two if we added internal absorption equivalent to $N(\text{H}) \sim 2 \times 10^{22} \text{ cm}^{-2}$. This neutral gas, along with the dust may be a wind seen in front of the nuclear engine (cf. Hönig et al. 2013).

Indeed, the $\text{H}\alpha/\text{H}\beta$ peak ratio in our spectra is ~ 20 and hence $\gg 2.8$ (as expected for Case B recombination; see Osterbrock 1974) and thus suggestive of differential extinction (reddening) by dust. A factor 7 differential extinction at these wavelengths corresponds to $E(B-V) \sim 1.6 \text{ mag}$ (cf. Lyu, Hao & Li 2014). With $N(\text{H}) \approx 2.2 \times 10^{21} A_V \text{ cm}^{-2}$ (Güver & Özel 2009) and a canonical $A_V \approx 3.1E(B-V)$ this would suggest an associated hydrogen column density $N(\text{H}) \sim 1 \times 10^{22} \text{ cm}^{-2}$. The factor two difference with the above estimate based on the X-ray attenuation can easily be accounted for by lowering the dust:gas ratio by a factor two compared to what is typical in the neutral ISM of the Milky Way, for instance if the gas is metal-poor (Tatton et al. 2013) or if it sublimates in the vicinity of the AGN. Thus, while each of the above determinations carries uncertainties in measurement and assumption, the fact that these independent measurements (X-ray, IR, optical lines) can be understood within a single, consistent picture lends credibility to the presence of a dusty X-ray absorber near to the central engine in SAGE0536AGN.

With a host galaxy stellar velocity dispersion of $\sigma = 123 \text{ km s}^{-1}$ we would have expected $M_{\text{BH}} \sim 1.8 \times 10^7 M_{\odot}$ (e.g., Ferrarese & Merritt 2000; Gebhardt et al. 2000; Tremaine et al. 2002; Gültekin et al. 2009; McConnell & Ma 2013). On

¹ <https://heasarc.gsfc.nasa.gov/cgi-bin/Tools/w3pimms/w3pimms.pl>

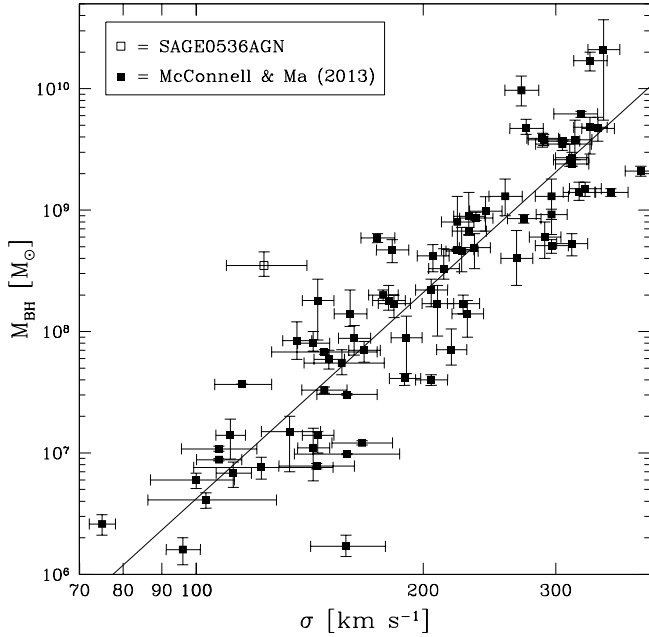


Figure 4. Black hole mass versus velocity dispersion. The McConnell & Ma (2013) sample are shown by filled symbols and their best-fit relation; their sample is a mixture of early- and late-type galaxies. SAGE0536AGN, indicated with the open symbol, is a clear outlier towards high black hole mass.

the basis of the estimated host galaxy mass we would have expected $M_{\text{BH}} \sim 5 \times 10^7 M_{\odot}$ (Sanghi et al. 2014). These are an order of magnitude below the $M_{\text{BH}} = 3.5 \pm 0.8 \times 10^8 M_{\odot}$ we determined for SAGE0536AGN; in figure 4 we plot the location of SAGE0536AGN in a $M_{\text{BH}}-\sigma$ diagram along with the data and best fit line from McConnell & Ma (2014). The latter consists of a mix of early- and late-type galaxies, but they do not differ much in their occupation of the diagram. Admittedly, the scatter around these relations is significant (Salviander & Shields 2013). The fact that SAGE0536AGN lies within a factor two of the $M_{\text{BH}}-M_{\text{spheroidal}}$ (Graham & Scott 2015) and $M_{\text{BH}}-L_{\text{spheroidal}}(V)$ (McConnell & Ma 2013; Park et al. 2015) relations may be regarded as confirmation that the host galaxy of SAGE0536AGN is indeed dominated by a spheroidal component. Over-massive black holes have been suggested in other galaxies, but these are based on luminosity determinations of the galaxy mass which depend on galaxy morphology; in the $M_{\text{BH}}-\sigma$ diagram they occupy unremarkable positions (Kormendy & Ho 2013).

McQuillin & McLaughlin (2013) explain the $M_{\text{BH}}-\sigma$ relation as resulting from self-regulated feedback, in which the black hole outflow speed, v_{outflow} features: $M_{\text{BH}}v_{\text{outflow}} \propto \sigma^5$ and thus any black hole outflow in SAGE0536AGN is expected to be weak, $v_{\text{outflow}} \sim 0.002 c$ compared to a median of $v_{\text{outflow}} \sim 0.035 c$ for local AGN (McQuillin & McLaughlin 2013). A slow outflow would also be consistent with the relatively high (for an AGN seen pole-on) hydrogen and dust column density as estimated above. Stronger winds in starbursts sometimes give rise to Na I D absorption (Rupke et al. 2005) but SAGE0536AGN is not a starburst galaxy and its Na I D profile shows no sign of significant broadening or displacement as one may expect from a strong wind.

The luminosity of the AGN can be determined from the $H\alpha$ luminosity (Woo et al. 2014):

$$\frac{L_{\text{bol}}(\text{AGN})}{10^{44} \text{ erg s}^{-1}} = 2.21 \times \left[\frac{L(H\alpha)}{10^{42} \text{ erg s}^{-1}} \right]^{0.86} \quad (3)$$

Hence we obtain $L_{\text{bol}}(\text{AGN}) = 5.3 \pm 0.4 \times 10^{45} \text{ erg s}^{-1}$. With an Eddington luminosity of $L_{\text{edd}} = 1.25 \times 10^{38} M(\text{BH}) \text{ erg s}^{-1}$ (Wyithe & Loeb 2002) we obtain $L_{\text{bol}}(\text{AGN})/L_{\text{edd}} = 0.12$. Hence the AGN in SAGE0536AGN is as active as one may expect for a black hole of this size – at high M_{BH} and $L_{\text{bol}}(\text{AGN})$ where almost all AGN are of optical type I (Oh et al. 2015).

Interestingly, the extreme silicate strength, moderately strong X-ray absorber and moderately high accretion rate are in fair agreement with models for an AGN comprising of a geometrically thin optically thick disc, geometrically thicker optically thinner medium (e.g., a disc wind) and an outflow cone for an inclination angle close to zero degrees (Stalevski et al. 2012; Schartmann et al. 2014).

4.3 An evolutionary picture

How can we explain the extreme properties of SAGE0536AGN? The modest star formation rate is typical of a radio-loud galaxy (Gürkan et al. 2015). Given the predominance of the BLR we could be looking into the heart of the AGN. The host is a rather modest-mass galaxy – not a giant cD elliptical galaxy such as M 87 of which the AGN is fed by cooling flows from the cluster inter-galactic medium. But SAGE0536AGN hosts a rather massive and actively accreting nuclear black hole. While the evidence we present here is in favour of a predominantly pressure-supported mature stellar system, we cannot fully rule out a lenticular galaxy with some rotational support, seen face-on – this could lower the observed velocity dispersion and bring it closer to the canonical $M_{\text{BH}}-\sigma$ relation.

The black hole in SAGE0536AGN could have been fed recently by a gas-rich minor merger or cooling flows from its circum-galactic environment. This would explain its current level of AGN activity for such modest galaxy host. Traces of intermediate-age populations in early-type galaxies of QSOs at redshifts $z \sim 0.2$ have recently been suggested to represent the aftermath of mergers (Canalizo & Stockton 2013), but no such intermediate-age populations are detected in SAGE0536AGN. Minor mergers have also been invoked to explain dust lanes in early-type galaxies, in which the star formation efficiency is very low (Davis et al. 2015). A merger scenario does not offer an explanation for the exuberant mass of the black hole, but black holes are in fact seen to grow at a faster rate than the galaxies they inhabit (Diamond-Stanic & Rieke 2012; LaMassa et al. 2013a), and galaxy growth may even be prematurely curtailed (Ferré-Mateu et al. 2015).

Nature appears to fine-tune the competition between circum-galactic cooling flows feeding a nuclear black hole or feeding star formation within the host galaxy, and the feedback from the black hole (and possibly star formation) heating the accreted gas thus preventing stars from forming. This balance relies critically on the timescales and development of thermal instabilities within the gas (Voit et al. 2015), and it may have shifted in the case of SAGE0536AGN towards

a relatively warm accretion flow and/or rapid feedback thus leading to black hole growth without the associated stellar mass build-up.

The AGN activity may now have largely subsided due to a lack of fresh fuel, having quenched all star formation in its host (cf. Stasińska et al. 2008; Cid Fernandes et al. 2010; Cimatti et al. 2013; Tasca et al. 2014; Wong et al. 2015). The black hole mass is now as massive as it gets, having devoured much of its host’s gas. It may resemble a lower-mass counterpart to the redshift 1.6 radio galaxy 5C 7.245 (Humphrey et al. 2015) or redshift 3.3 galaxy CID-947 (Trakhtenbrot et al. 2015); the lower redshift at which we see something similar happen to SAGE0536AGN is in agreement with the ‘downsizing’ scenario in which lower-mass galaxies evolve more slowly. Galaxies with $M_{\text{stars}} \sim 2.5 \times 10^{10} M_{\odot}$ are indeed seen to be nearing the end of their assembly history around redshift $z \sim 0.1\text{--}0.2$ (McDermid et al. 2015). However, the old age of SAGE0536AGN (> 9 Gyr, i.e. $z > 2.25$) seems incompatible with this evolutionary scenario. Interestingly, some nearby star-forming dwarf galaxies with broad-line AGN have been found with M_{BH} about seven times that expected from the $M_{\text{BH}}\text{--}M_{\text{stars}}$ relation (viz. galaxies B and D in Reines, Greene & Geha 2013). The latter could represent even more delayed transformation of even lower-mass AGN-host galaxies, again consistent with the mass-dependent galaxy assembly history paradigm (McDermid et al. 2015). On the other hand, this would fail to explain the over-massive black hole in the nearby *massive* lenticular galaxy NGC 1277 (Scharwächter et al. 2015).

The effective radius R_e of the host galaxy may be the parameter which improves upon the $M_{\text{BH}}\text{--}\sigma$ relation to create a fundamental plane of $M_{\text{BH}}\text{--}\sigma\text{--}R_e$ (Marconi & Hunt 2003; de Francesco, Capetti & Marconi 2006). If SAGE0536AGN is in transformation from a late-type to an early-type galaxy, its effective radius may now be relatively large. This would be expected for newly quenched early-type galaxies (Daddi et al. 2005; Trujillo et al. 2007; Carollo et al. 2013; Cassata et al. 2013; Poggianti et al. 2013), but SAGE0536AGN appears to have stopped forming stars in abundance already some 9 Gyr ago.

Much to the contrary, Katkov, Kniazev & Sil’chenko (2015) suggest lenticular galaxies are only now building up discs that may see them eventually transform into spiral galaxies. The mechanism for this transformation is accretion of cold gas from their surroundings, which could indeed fuel also a nuclear black hole. The large spread in ages for lenticular (S0) galaxies (Poggianti et al. 2001, 2009) – which have σ broadly similar to that of SAGE0536AGN – indicates that this process may still be on-going at $z < 1$. While it does not explain the large black hole mass in SAGE0536AGN, aside from its low σ possibly being due to projection effects it could also mean that SAGE0536AGN may evolve closer to the canonical $M_{\text{BH}}\text{--}\sigma$ relation as the galaxy grows in mass (cf. DeGraf et al. 2015). On the other hand, there is no evidence of stars younger than ~ 9 Gyr in the optical spectrum of SAGE0536AGN, which seems to be in tension with it building up a disc now.

An alternative explanation for super-massive black holes was offered by Volonteri & Ciotti (2013) for central cluster galaxies, which they suggest are predominantly the result from dry mergers that do little to increase the velocity dispersion. Savorgnan & Graham (2015) found a lack

of evidence for this scenario among massive galaxies. That does not mean that it may not be a viable option for less massive galaxies such as SAGE0536AGN. It could explain why it lies closer to the $M_{\text{BH}}\text{--}M_{\text{spheroid}}$ relation than to the $M_{\text{BH}}\text{--}\sigma$ relation.

There must be other objects like SAGE0536AGN, and these could well form a new sub-class of weak-line radio galaxies (WLRG) with warm dust. WLRG galaxies are defined by their optical [O III] equivalent width $< 10 \text{ \AA}$ (Tadhunter et al. 1998); they are not normally associated with dust and it has therefore been suggested that they may be accreting directly from the hot inter-galactic medium (Hardcastle, Evans & Croston 2007). SAGE0536AGN would classify as a WLRG, but it does contain dust. Another WLRG, PKS 0043–42 at $z = 0.116$ (Tadhunter et al. 1993) also exhibits warm dust, though with $F_{70}/F_{24} = 0.9$ it is less extreme than SAGE0536AGN. While in PKS 0043–42 the silicate is seen in absorption (Ramos Almeida et al. 2011) and it is a FR-II object, these differences with SAGE0536AGN could be largely explained by orientation effects with PKS 0043–42 being seen edge on.

5 CONCLUSIONS

Optical spectra obtained with the SALT have allowed us to better characterise the peculiar AGN-dominated galaxy SAGE1C J053634.78–722658.5 (SAGE0536AGN for short):

- We determine an accurate redshift of $z = 0.1428 \pm 0.0001$ from the optical absorption and emission lines.
- We confirm the strong presence of an AGN, of type I based on broad H α emission.
- We determine the black hole mass $M_{\text{BH}} \sim 3.5 \pm 0.8 \times 10^8 M_{\odot}$, on the basis of the H α width and luminosity, accreting at ~ 12 per cent of the Eddington rate.
- Narrower, weaker H α and [N II] emission is attributed to the NLR around the AGN; limits on the far-IR emission rule out a star formation origin of the line emission.
- The overall appearance of the optical spectrum is that of an early-type galaxy at least ~ 9 Gyr old, consistent with the absence of star formation indicators.
- We measure a stellar velocity dispersion $\sigma = 123 \pm 15 \text{ km s}^{-1}$ and hence derive a host galaxy mass $M_{\text{stars}} \sim 2.5_{1.2}^{2.5} \times 10^{10} M_{\odot}$.
- The mid-IR properties, in particular the intense silicate emission, point towards an AGN torus seen close to pole-on but with moderate X-ray absorption possibly associated with a dusty wind.
- SAGE0536AGN lies (well) above the canonical $M_{\text{BH}}\text{--}\sigma$ and $M_{\text{BH}}\text{--}M_{\text{stars}}$ relations, explaining its original discovery by Hony et al. (2011) as an AGN-dominated galaxy.

Outliers like SAGE0536AGN may provide useful clues as to how the observed scaling relations arise and evolve. SAGE0536AGN will need to accumulate stellar mass in future, if it is going to move closer to the main scaling relations between M_{BH} and host galaxy properties. But it does not appear to have an internal reservoir of gas to do so.

Deep, high-resolution optical images of the host galaxy are needed to confirm its morphological type and to determine the effective radius – to improve the determination of

the mass of the spheroidal component – thus elucidating the nature and evolutionary status of this remarkable galaxy.

ACKNOWLEDGMENTS

We would like to thank Poshak Gandhi for discussions regarding the X-ray data, and the referee, Daniel Dicken, for a positive report and queries which have helped us to clarify some of our reasoning. All of the observations reported in this paper were obtained with the Southern African Large Telescope (SALT). Keele University and the University of Central Lancashire form part of the United Kingdom SALT Consortium, a partner in SALT. This publication makes use of data products from the Wide-field Infrared Survey Explorer, which is a joint project of the University of California, Los Angeles, and the Jet Propulsion Laboratory/California Institute of Technology, funded by the National Aeronautics and Space Administration. This research has made use of the SIMBAD database, operated at CDS, Strasbourg, France.

REFERENCES

- Alatalo K., Cales S. L., Appleton P. N., Kewley L. J., Lacy M., Lisenfeld U., Nyland K., Rich J. A., 2014, *ApJ*, 794, L13
- Antonucci R., 1993, *ARA&A*, 31, 473
- Antonucci R. R. J., Miller J. S., 1985, *ApJ*, 297, 621
- Baldwin J. A., Phillips M. M., Terlevich R., 1981, *PASP*, 93, 5
- Balogh M. L., Morris S. L., Lee H. K. C., Carlberg R. G., Ellingson E., 1999, *ApJ*, 527, 54
- Beckmann V., Shradler C. R., 2012, *Active Galactic Nuclei*, Wiley–VCH Verlag GmbH
- Belli S., Newman A. B., Ellis R. S., 2014, *ApJ*, 783, 117
- Bouquin A. Y. K., 2015, *ApJ*, 800, L19
- Buckley D. A. H., Swart G. P., Meiring J. G., 2006, *SPIE*, 6267, 32
- Burgh E. B., Nordsieck K. H., Kobulnicky H. A., Williams T. B., O’Donoghue D., Smith M. P., Percival J. W., 2003, *SPIE*, 4841, 1463
- Canalizo G., Stockton A., 2013, *ApJ*, 772, 132
- Cappellari M., Emsellem E., 2004, *PASP*, 116, 138
- Cappellari M., et al., 2013, *MNRAS*, 432, 1862
- Carollo C. M., et al., 2013, *ApJ*, 773, 112
- Cassata P., et al., 2013, *ApJ*, 775, 106
- Cid Fernandes R., Stasińska G., Schlickmann M. S., Mateus A., Vale Asari N., Schoenell W., Sodré L., 2010, *MNRAS*, 403, 1036
- Cimatti A., et al., 2013, *ApJ*, 779, L13
- Cluver M. E., et al., 2014, *ApJ*, 782, 90
- Crawford S. M., et al., 2010, *SPIE*, 7737, 82
- Cutri, R. M., et al., 2014, *VizieR On-line Data Catalog: II/328*
- Daddi E., et al., 2005, *ApJ*, 626, 680
- Davis T. A., et al., 2015, *MNRAS*, 449, 3503
- de Francesco G., Capetti A., Marconi A., 2006, *A&A*, 460, 439
- DeGraf C., Di Matteo T., Treu T., Feng Y., Woo J.-H., Park D., arXiv:1412.4133
- Diamond-Stanic A. M., Rieke G. H., 2012, *ApJ*, 746, 168
- Dicken D., Tadhunter C., Morganti R., Buchanan C., Oosterloo T., Axon D., 2008, *ApJ*, 678, 712
- Dicken D., Tadhunter C., Axon D., Robinson A., Morganti R., Kharb P., 2010, *ApJ*, 722, 1333
- Dicken D., et al., 2014, *ApJ*, 788, 98
- Fanaroff B. L., Riley J. M., 1974, *MNRAS*, 167, P31
- Ferrarese F., Merritt D., 2000, *ApJ* 539, L9
- Ferré-Mateu A., Mezcua M., Trujillo I., Balcells M., van den Bosch R. C. E., arXiv:1506.02663
- Fukugita M., Ichikawa T., Gunn J. E., Doi M., Shimasaku K., Schneider D. P., 1996, *AJ*, 111, 1748
- Gandhi P., Horst H., Smette A., Höing S., Comastri A., Gilli R., Vignali C., Duschl W., 2009, *A&A*, 502, 457
- Gebhardt K., et al., 2000, *ApJ*, 539, L13
- Graham A. W., 2015, in: “Galactic Bulges”, eds. E. Laurikainen, R. F. Peletier & D. A. Gadotti (Springer), arXiv:1501.02937
- Graham A. W., Scott N., 2015, *ApJ*, 798, 54
- Groves B. A., et al., 2015, *ApJ*, 799, 96
- Gruendl R. A., Chu Y.-H., 2009, *ApJS*, 184, 172
- Gültekin K., et al., 2009, *ApJ*, 698, 198
- Gürkan G., et al., 2015, arXiv:1507.01552
- Güver T., Özel F., 2009, *MNRAS*, 400, 2050
- Hardcastle M. J., Evans D. A., Croston J. H., 2007, *MNRAS*, 376, 1849
- Höing S. F., et al., 2013, *ApJ*, 771, 87
- Hony S., et al., 2011, *A&A*, 531, 137 (H11)
- Hopkins A. M., et al., 2003, *ApJ*, 599, 971
- Humphrey A., et al., 2015, *MNRAS*, 447, 3322
- Kaspi S., Smith P. S., Netzer H., Maoz D., Jannuzi B. T., Giveon U., 2000, *ApJ*, 533, 631
- Katkov I. Yu., Kniazev A. Yu., Sil’chenko O. K., 2015, *AJ*, 150, 24
- Kauffmann G., et al., 2003a, *MNRAS*, 341, 33
- Kauffmann G., et al., 2003b, *MNRAS*, 346, 1055
- Kellermann K. I., Sramek R., Schmidt M., Shaffer D. B., Green R., 1989, *AJ*, 98, 1195
- Kemper F., et al., 2010, *PASP*, 122, 683
- Kewley L. J., Heisler C. A., Dopita M. A., Lumsden S., 2001, *ApJS*, 132, 37
- Kobulnicky H. A., Nordsieck K. H., Burgh E. B., Smith M. P., Percival J. W., Williams T. B., O’Donoghue D., 2003, *SPIE*, 4841, 1634
- Kormendy J., Ho L. C., 2013, *ARA&A*, 51, 511
- LaMassa S. M., Heckman T. M., Ptak A., Urry C. M., 2013a, *ApJ*, 765, L33
- LaMassa S. M., et al., 2013b, *MNRAS*, 436, 3581
- Lyu J., Hao L., Li A., 2014, *ApJ*, 792, L9
- Marconi A., Hunt L. K., 2003, *ApJ*, 589, L21
- McConnell N. J., Ma C.-P., 2013, *ApJ*, 764, 184
- McDermid R. M., et al., 2015, *MNRAS*, 448, 3484
- McQuillin R. C., McLaughlin D. E., 2013, *MNRAS*, 434, 1332
- Meixner M., et al., 2006, *AJ*, 132, 2268
- Netzer H., 2015, *ARA&A*, 53
- Oh K., Yi S. K., Schawinski K., Koss M., Trakhtenbrot B., Soto K., 2015, *ApJS*, 219, 1
- Osterbrock D. E., 1974, *Astrophysics of Gaseous Nebulae*, W.H. Freeman and Company
- Osterbrock D. E., 1977, *ApJ*, 215, 733
- Osterbrock D. E., 1981, *ApJ*, 249, 462
- Park D., Woo J.-H., Bennert V. N., Treu T., Auger M. W., Malkan M. A., 2015, *ApJ*, 799, 164
- Planck Collaboration, 2015, arXiv:1502.01589
- Poggianti B. M., et al., 2001, *ApJ*, 563, 118
- Poggianti B. M., et al., 2009, *ApJ*, 697, L137
- Poggianti B. M., et al., 2013, *ApJ*, 762, 77
- Ramos Almeida C., Dicken D., Tadhunter C., Asensio Ramos A., Inskip K. J., Hardcastle M. J., Mingo B., 2011, *MNRAS*, 413, 2358
- Reines A. E., Greene J. E., Geha M., 2013, *ApJ*, 775, 116
- Renzini A., Peng Y., 2015, *ApJ*, 801, L29
- Rose M., Tadhunter C. N., Holt J., Rodríguez Zaurín J., 2013, *MNRAS*, 432, 2150
- Rupke D. S., Veilleux S., Sanders D. B., 2005, *ApJ*, 632, 751
- Salviander S., Shields G. A., 2013, *ApJ*, 764, 80

- Sanghvi J., Kotilainen J. K., Falomo R., Decarli R., Karhunen K., Uslenghi M., 2014, *MNRAS*, 445, 1261
- Savorgnan G. A. D., Graham A. W., 2015, *MNRAS*, 446, 2330
- Schartmann M., Wada K., Prieto M. A., Burkert A., Tristram K. R. W., 2014, *MNRAS*, 445, 3878
- Scharwächter J., Combes F., Salomé P., Sun M., Krips M., arXiv:1507.02292
- Schmidt M., Green R. F., 1983, *ApJ*, 269, 352
- Spoon H. W. W., Marshall J. A., Houck J. R., Elitzur M., Hao L., Armus L., Brandl B. R., Charmandaris V., 2007, *ApJ*, 654, L49
- Stalevski M., Fritz J., Baes M., Nakos T., Popović L. Č., 2012, *MNRAS*, 420, 2756
- Stasińska G., Vale Asari N., Cid Fernandes R., Gomes J. M., Schlickmann M., Mateus A., Schoenell W., Sodré L., 2008, *MNRAS*, 391, L29
- Staveley-Smith L., Kim S., Calabretta M. R., Haynes R. F., Kesteven M. J., 2003, *MNRAS*, 339, 87
- Tadhunter C. N., Morganti R., di Serego-Alighieri S., Fosbury R. A. E., Danziger I. J., 1993, *MNRAS*, 263, 999
- Tadhunter C. N., Morganti R., Robinson A., Dickson R., Villar-Martin M., Fosbury R. A. E., 1998, *MNRAS*, 298, 1035
- Tasca L. A. M., et al., 2014, *A&A*, 564, L12
- Tatton B. L., et al., 2013, *A&A*, 554, 33
- Trakhtenbrot B., et al., 2015, *Science*, 349, 168
- Tremaine S., et al., 2002, *ApJ*, 574, 740
- Trujillo I., Conselice C. J., Bundy K., Cooper M. C., Eisenhardt P., Ellis R. S., 2007, *MNRAS*, 382, 109
- Urry M., Padovani P., 1995, *PASP*, 107, 803
- van Loon J. Th., et al., 2013, *A&A*, 550, 108
- Vestergaard M., Peterson B. M., 2006, *ApJ*, 641, 689
- Voit G. M., Bryan G. L., O'Shea B. W., Donahue M., 2015, arXiv:1505.03592
- Volonteri M., Ciotti L., 2013, *ApJ*, 768, 29
- Vulcani B., Poggianti B. M., Fritz J., Fasano G., Moretti A., Calvi R., Paccagnella A., 2015, *ApJ*, 798, 52
- Wake D. A., van Dokkum P. G., Franx M., 2012, *ApJ*, 751, L44
- Wijesinghe D. B., et al., 2011, *MNRAS*, 410, 2291
- Willott C. J., Bergeron J., Omont A., 2015, *ApJ*, 801, 123
- Wong O. I., Schawinski K., Józsa G. I. G., Urry C. M., Lintott C. J., Simmons B. D., Kaviraj S., Masters K. L., 2015, *MNRAS*, 447, 3311
- Woo J.-H., Kim J.-G., Park D., Bae H.-J., Kim J.-H., Lee S.-E., Kim S. C., Kwon H.-J., 2014, *JKAS*, 47, 167
- Woods P.M., et al., 2011, *MNRAS*, 411, 1597
- Worthey G., Ottaviani D. L., 1997, *ApJS*, 111, 377
- Wuyts S., et al., 2012, *ApJ*, 753, 114
- Wyithe J. S. B., Loeb J., 2002, *ApJ*, 581, 886
- Yang X.-H., Chen P.-S., Huang Y., 2015, *MNRAS*, 449, 3191